JOURNAL OF SOLID STATE CHEMISTRY 119, 164–168 (1995)

Surface Characterization of $LaMnO_{3+\delta}$ Powder Annealed in Air

Hideki Taguchi,[1] Akio Sugita, and Mahiko Nagao

Research Laboratory for Surface Science, Faculty of Science, Okayama University, Okayama 700, Japan

and

Kenji Tabata

Research Institute of Innovation Technology for the Earth (RITE), Kizugawadai, Kizu-cho, Soraku-gun, Kyoto 619-02, Japan

Received January 30, 1995; in revised form May 25, 1995; accepted May 25, 1995

Perovskite-type $LaMnO_{3+\delta}$, synthesized using poly(acrylic acid) (PAA), was annealed at 400 and 700°C in air for 6–54 hr. The crystallite size, the specific surface area, the La/Mn ratio, and the catalytic activity of $LaMnO_{3+\delta}$ were measured to characterize the surface. The specific surface area decreased slightly with increasing annealing time, while the La/Mn ratio of the surface, calculated from the XPS measurements, was independent of annealing time. The catalytic activity for the oxidation of CO increased with annealing. These results suggest that annealing improved the crystallinity (regularity of the ions) of the $LaMnO_{3+\delta}$ surface.

INTRODUCTION

Recently, there has been an interest in examining the oxidation of hydrocarbons on perovskite-type oxides (1–5). $LaMO_3$ (M = Cr, Mn, Fe, Co, and Ni) shows a high activity for the oxidation of carbon monoxide (CO). The catalytic activity for the oxidation of CO on $LaNiO_3$ is higher than that on NiO (6). $LaMO_3$ is generally synthesized at high temperature, using a standard ceramic technique. Therefore, the oxides sinter and the specific surface area of $LaMO_3$ is less than 5 m^2/g (2, 3). To improve the catalytic activity, it is necessary to synthesize $LaMO_3$ with a large specific surface area.

Perovskite-type $(La_{1-x}Sr_x)MnO_3$ was synthesized at low temperature using poly(acrylic acid) (PAA), and the specific surface area of $(La_{1-x}Sr_x)MnO_3$ was ca. 18–24 m^2/g (7). Recently, we noticed that the crystal structure and the oxygen content of $(La_{1-x}Sr_x)MnO_3$ depended strongly on the PAA concentration of the gel. Therefore, we synthesized $LaMnO_{3+\delta}$ (x = 0) at low temperature using gels with various PAA concentrations, and examined the relation between the PAA concentration, the crystal structure, and the oxygen content (8). In case of the low PAA concentration, the oxygen content was nearly 3.00 and the crystal structure was orthorhombic. With increasing PAA concentration, the oxygen content increased to ca. 3.17 and the crystal structure changed from orthorhombic to hexagonal.

PAA burns below 300°C as shown by a thermal analysis (DTA), and the combustion heat of PAA causes a rapid increase in temperature (7). The rapid changes in temperature caused a large number of cracks in $LaMnO_{3+\delta}$, resulting in a large specific surface area (9). In the present study, $LaMnO_{3+\delta}$ synthesized using PAA was annealed at 400 and 700°C in air for 6–54 hr to improve the crystallinity (the regularity of the ions) of the surface. X-ray photoelectron spectroscopy (XPS) measurements were performed to determine the chemical composition of the $LaMnO_{3+\delta}$ surface. The specific surface area and the catalytic activity for the oxidation of CO were measured. These results will provide information for characterizing the $LaMnO_{3+\delta}$ surface.

EXPERIMENTAL

The preparation of $LaMnO_{3+\delta}$ with PAA has been described in detail elsewhere (8). In the present study, the PAA concentration was 2×10^{-2} M. The gel was fired at 400 and 700°C in air for 6–54 hr. The phases of the samples were identified by X-ray powder diffraction (XRD) using monochromatic Cu$K\alpha$ radiation. The oxygen content in each sample was determined by an oxygen–reduction (redox) method (8). The XPS measurements were carried out for the La3d, Mn2p, O1s, and C1s levels of the samples using Mg$K\alpha$ radiation at room temperature. The binding energy was calibrated using the C1s level from the usual contamination. The specific surface area of the samples was determined by the BET method for nitrogen adsorption. The catalytic activities for the oxidation of

[1] To whom correspondence should be addressed.

0022-4596/95 $12.00

TABLE 1

Oxygen Content ($3 + \delta$), Crystallite Size (D_{122}), Specific Surface Area (S) of Annealed $LaMnO_{3+\delta}$, and Rate of Reaction (R) of $LaMnO_{3+\delta}$ for the Oxidation of CO at 270°C

Annealing condition					
Temperature (°C)	Time (hr)	$3 + \delta$	D_{122} (nm)	S (m^2/g)	R ($cm^3\ min^{-1}\ m^{-2}$)
400	6	3.13	9.3	26.9	0.070
400	30	3.20	11.1	28.0	0.109
400	54	3.21	11.1	25.4	0.122
700	6	3.13	11.8	23.5	0.213
700	30	3.20	12.7	15.7	0.295

CO were measured at 195 to 300°C using a conventional flow system. The samples (0.2 g) were preheated at 300°C under a pure oxygen stream for 3 hr. A mixed gas of CO (1.0%), O_2 (4.0%), and He (balance) was fed in a flow reactor at a flow rate of 150 $cm^3 \cdot min^{-1}$. The products were analyzed by gas chromatography using a column (Molecular Sieve 5A) kept at 50°C during the measurements.

RESULTS AND DISCUSSION

XRD patterns of the samples annealed at 400 and 700°C in air for 6–54 hr were indexed as the hexagonal perovskite-type structure. The relation between the oxygen content ($3 + \delta$) of $LaMnO_{3+\delta}$ and the annealing condition (temperature and time) is shown in Table 1. With an increase in annealing time, the oxygen content increased to ca. 3.20. We calculated the crystallite size (D_{122}) of $LaMnO_{3+\delta}$ from the full width at half-maximum (FWHM) of a diffraction peak (122) using the Scherrer formula (10). The relation between D_{122} and the annealing condition (temperature and time) is shown in Table 1. D_{122} increased slightly with increasing annealing time. At a certain annealing time, D_{122} of $LaMnO_{3+\delta}$ annealed at 700°C was larger than that annealed at 400°C. The relation between the specific surface area of $LaMnO_{3+\delta}$ and the annealing condition is shown in Table 1. The specific surface area of $LaMnO_{3+\delta}$ annealed at 400°C decreased slightly with increasing annealing time. As for $LaMnO_{3+\delta}$ annealed at 700°C, the specific surface area decreased from ca. 23.5 to ca. 15.7 m^2/g. From the results of Table 1, it is considered that the crystal growth or the sintering of $LaMnO_{3+\delta}$ occurred upon annealing, with the result that the number of cracks on the $LaMnO_{3+\delta}$ surface decreased.

The XPS spectra of the La3$d_{5/2}$, Mn2$p_{3/2}$, O1s, and C1s levels of $LaMnO_{3+\delta}$ are shown in Figs. 1, 2, 3, and 4, respectively. A satellite peak was observed to the high binding energy side of the main La3$d_{5/2}$ peaks by ca. 4

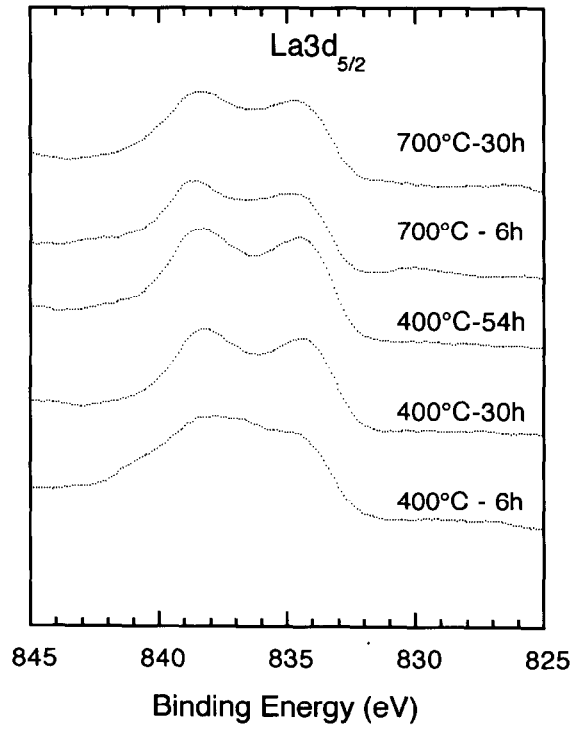

FIG. 1. The XPS spectra of the La3$d_{5/2}$ level of $LaMnO_{3+\delta}$ annealed at 400 and 700°C in air for 6–54 hr.

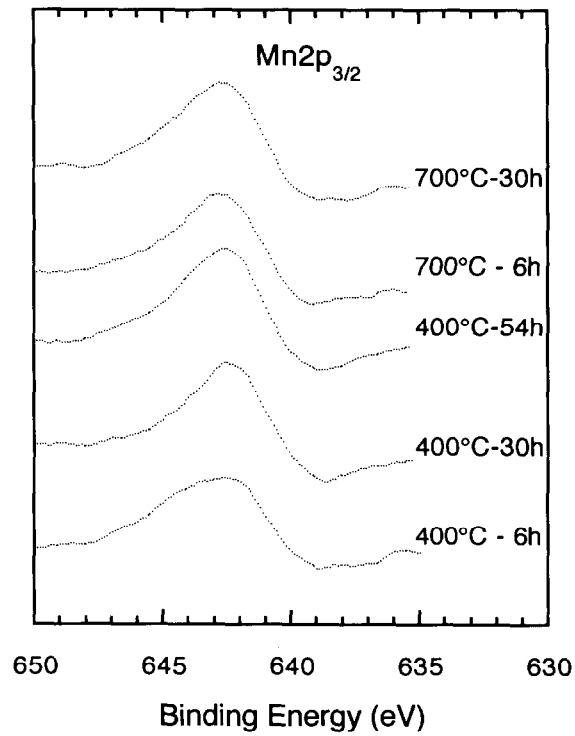

FIG. 2. The XPS spectra of the Mn2$p_{3/2}$ level of $LaMnO_{3+\delta}$ annealed at 400 and 700°C in air for 6–54 hr.

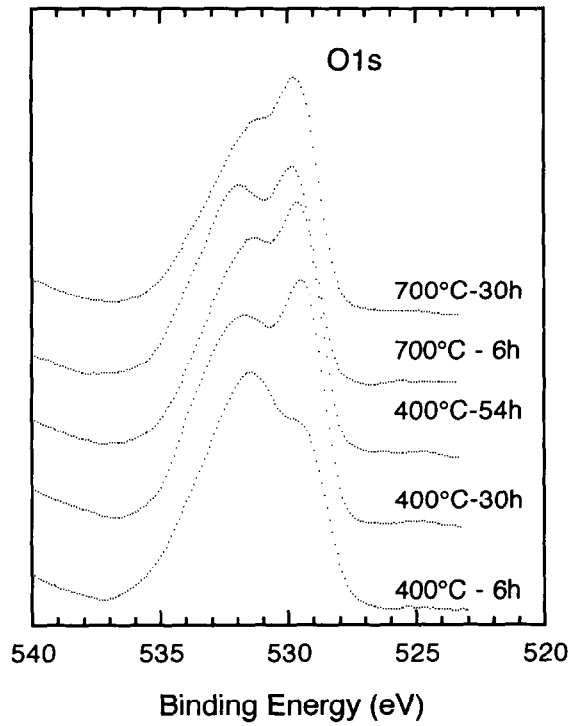

FIG. 3. The XPS spectra of the O1s level of $LaMnO_{3+\delta}$ annealed at 400 and 700°C in air for 6–54 hr.

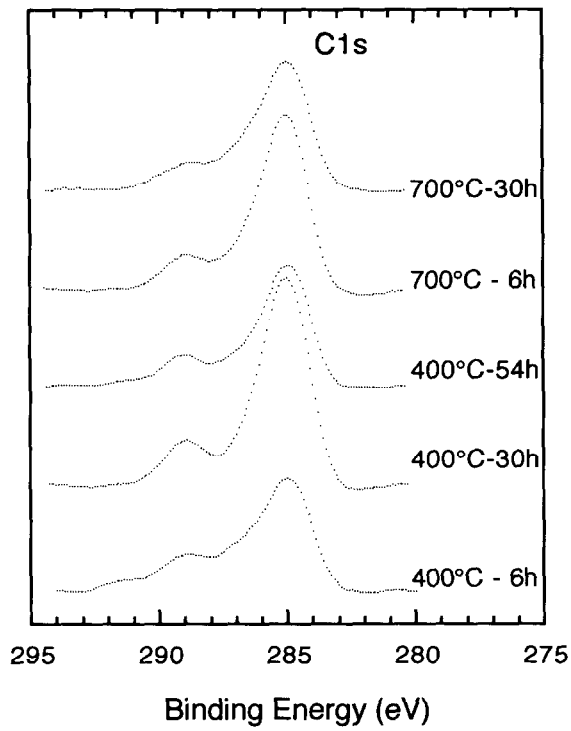

FIG. 4. The XPS spectra of the C1s level of $LaMnO_{3+\delta}$ annealed at 400 and 700°C in air for 6–54 hr.

TABLE 2
Binding Energies of La3$d_{5/2}$ and Mn2$p_{3/2}$ Levels of $LaMnO_{3+\delta}$

Annealing condition		La3$d_{5/2}$	FWHM	Mn2$p_{3/2}$	FWHM
Temperature (°C)	Time (hr)	(eV)	(eV)	(eV)	(eV)
400	6	834.9	3.1	642.5	4.6
400	30	834.3	2.2	642.5	3.6
400	54	834.5	2.5	642.4	3.8
700	6	834.7	2.5	642.8	3.9
700	30	834.7	2.9	642.8	4.0

eV. This satellite was interpreted as the excitation of an electron from the anion valence band into the lanthanum f band (11). The Mn2$p_{3/2}$ level is broad, and asymmetric toward the high binding energy site. The binding energies of the La3$d_{5/2}$ and Mn2$p_{3/2}$ levels are shown in Table 2, and were independent of the annealing condition: 834.6 ± 0.3 eV for the La3$d_{5/2}$ level and 642.6 ± 0.2 eV for the Mn2$p_{3/2}$ level. Although the oxygen content of $LaMnO_{3+\delta}$ increased with increasing annealing time, as shown in Table 1, we could not observe a large variation in both the binding energies and FWHM of the La3$d_{5/2}$ and Mn2$p_{3/2}$ levels, except for that of $LaMnO_{3+\delta}$ annealed at 400°C for 6 hr. The O1s level has two peaks, and these peaks are independent of the annealing condition. The lower binding peak is ca. 529.7 eV and assignable to a lattice oxygen. The higher binding peak is ca. 531.5 eV and assignable to an adsorbed oxygen or hydroxyl group (12, 13). The C1s level has two peaks: one is the contaminated carbon (285.0 eV), and another small peak near 289.0 eV is considered to be carbonate (14). Because La-based perovskites are basic materials, $LaMnO_{3+\delta}$ is easily carbonated by moisture that yields high binding energy of O1s.

Taguchi *et al.* discussed the chemical bonding of orthorhombic perovskite-type $(Nd_{1-x}Ca_x)MnO_3$ with respect to the binding energy (15). The binding energies of the Nd4d, the Ca2p, and the O1s levels decreased with increasing x. The variation in the binding energy was due to the partial ionic character of Nd and Ca. In the present study, the constant binding energies of the La3$d_{5/2}$ and the Mn2$p_{3/2}$ levels suggest that the chemical bonding for $LaMnO_{3+\delta}$ was not affected by the annealing condition. We calculated the La and the Mn contents of the $LaMnO_{3+\delta}$ surface from the intensities of the La3$d_{5/2}$ and the Mn2$p_{3/2}$ levels (9). The relation between the La/Mn ratio of the $LaMnO_{3+\delta}$ surface and the annealing condition is shown in Fig. 5. Although the crystallite size (D_{122}) and the specific surface area of $LaMnO_{3+\delta}$ depended on annealing time, the La/Mn ratio of the $LaMnO_{3+\delta}$ surface was independent of annealing time. With increasing an-

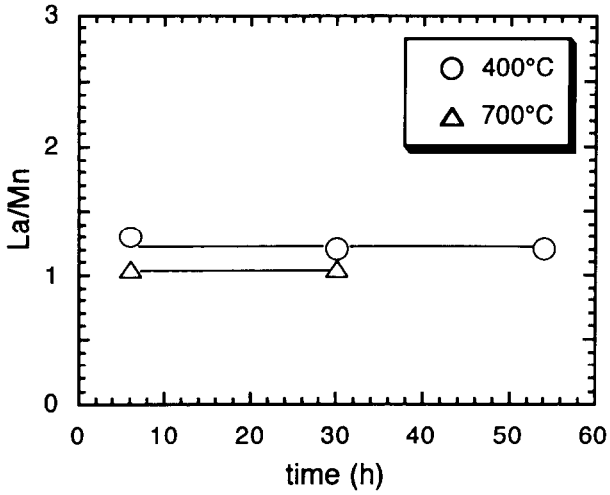

FIG. 5. The La/Mn ratio of the $LaMnO_{3+\delta}$ surface vs the annealing condition. The La/Mn ratio was calculated by the XPS measurements.

nealing temperature, the chemical composition of the $LaMnO_{3+\delta}$ surface approached the stoichiometric value (La/Mn = 1.0).

The conversion from CO to CO_2 was measured for the various $LaMnO_{3+\delta}$ samples. Figure 6 shows the conversion on $LaMnO_{3+\delta}$ annealed at 400°C for 6 and 54 hr. Although the specific surface area of $LaMnO_{3+\delta}$ decreased slightly with increasing annealing time as seen in Table 1, the catalytic activity of $LaMnO_{3+\delta}$ annealed for 54 hr was larger than that annealed for 6 hr. These results indicate that there is an important factor, other than the large specific surface area, for improvement of the catalytic activity for the oxidation of CO. The rate of reaction (R) at a given temperature is calculated using the equation

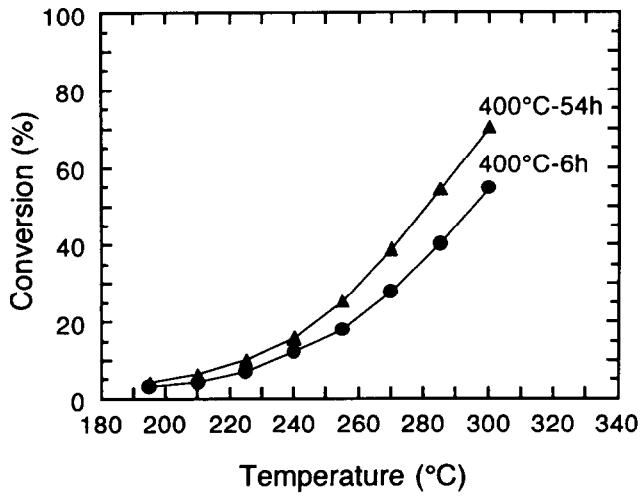

FIG. 6. The conversion from CO to CO_2 on $LaMnO_{3+\delta}$ annealed at 400°C in air for 6 and 54 hr.

$$R = \frac{F \times C \times \mathrm{Cv}}{m \times S},$$

where F is the gas flow per minute, C is the initial concentration of CO, Cv is the conversion per gram from CO to CO_2, m is the mass of the sample, and S is the specific surface area of the sample (16). The relation between R at 270°C and the annealing condition is shown in Table 1. R increased with increasing annealing time or annealing temperature.

According to the results reported by Voorhoeve *et al.* (17), the oxidation of CO occurs at the metal ions of the surface. Both the metal ion content and the surface crystallinity play important roles in the catalytic activity. There are two kinds of oxygen at the surface: one is lattice oxygen, and the other is oxygen adsorbed on the metal ions. CO_2 is produced by the reaction of CO with oxygen adsorbed on the metal ions of the outermost surface. After the desorption of CO_2 from the surface, oxygen is again adsorbed on the metal ions. In the present study, although the Mn ion content of the $LaMnO_{3+\delta}$ surface was independent of annealing time and the specific surface area of $LaMnO_{3+\delta}$ decreased with annealing, the catalytic activity for the oxidation of CO increased. From these results, it is considered that annealing improved the crystallinity of the $LaMnO_{3+\delta}$ surface, and that the measurement of the catalytic activity is an important method for estimating the crystallinity of the $LaMnO_{3+\delta}$ surface. To discuss the surface crystallinity, it will be necessary to observe the $LaMnO_{3+\delta}$ surface by high-resolution electron microscopy (HREM) in the near future.

CONCLUSION

The crystallite size of $LaMnO_{3+\delta}$ increased slightly with annealing. The binding energies of the La3$d_{5/2}$, Mn2$p_{3/2}$, and O1s levels from the XPS measurements were independent of the annealing condition, and the chemical bonding of $LaMnO_{3+\delta}$ was not affected by the annealing condition. The La/Mn ratio of the $LaMnO_{3+\delta}$ surface was independent of the annealing time, while the catalytic activity for the oxidation of CO increased with annealing time. These results suggest that the crystallinity of the $LaMnO_{3+\delta}$ surface is important in obtaining high catalytic activity for the oxidation of CO.

ACKNOWLEDGMENTS

The authors express their thanks to S. Matsu-ura for the chemical analysis and M. Kamada for assistance with the XPS measurements. This work was partly supported by NEDO (New Energy and Industrial Technology Development Organization, Japan).

REFERENCES

1. L. G. Tejuca, J. G. Fierro, and J. M. D. Tascon, *Adv. Catal.* **36,** 237 (1989).

2. T. Nitadori, S. Kurihara, and M. Misono, *J. Catal.* **98,** 221 (1986).
3. K. Tabata, I. Matsumoto, and S. Kohiki, *J. Mater. Sci.* **22,** 1882 (1987).
4. T. Nitadori, T. Ichiki, and M. Misono, *Bull. Chem. Soc. Jpn.* **61,** 621 (1988).
5. N. Mizuno, M. Tanaka, and M. Misono, *J. Chem Soc. Faraday Trans.* **88,** 91 (1992).
6. T. Seiyama, "Metal Oxides and Catalysis," p. 211, Koudan-Sha, Tokyo, 1979.
7. H. Taguchi, D. Matsuda, M. Nagao, K. Tanihata, and Y. Miyamoto, *J. Am. Ceram. Soc.* **75,** 201 (1992).
8. H. Taguchi, H. Yoshioka, D. Matsuda, and M. Nagao, *J. Solid State Chem.* **104,** 460 (1993).
9. H. Taguchi, H. Yoshioka, M. Nagao, and Y. Takeda, *J. Solid State Chem.* **116,** 343 (1995).
10. B. D. Cullity, "Elements of X-Ray Diffraction," p. 102. Addison–Wesley, London, 1978.
11. D. J. Lam, B. W. Veal, and D. E. Ellis, *Phys. Rev. B* **22,** 5730 (1972).
12. K. Tabata, and S. Kohiki, *Bull. Chem. Soc. Jpn.* **65,** 1295 (1992).
13. Y. Wu, J. T. Mayer, E. Garfunkel, and T. E. Madey, *Langmuir* **10,** 1482 (1994).
14. R. Mariscal, J. Soria, M. A. Pena, and J. L. G. Fierro, *J. Catal.* **147,** 535 (1994).
15. H. Taguchi, M. Nagao, M. Shimada, Y. Takeda, and O. Yamamoto, *J. Solid State Chem.* **77,** 336 (1988).
16. Y. Ogino, T. Onoda, S. Shikagawa, M. Karube, Y. Saito, K. Tabe, T. Tamura, H. Matsumoto, M. Misono, and K. Yoshida, "Catalysis," p. 880, Maruzen, Tokyo, 1986.
17. R. H. Voorhoeve, D. W. Johnson, J. P. Remeika, and P. K. Gallagher, *Science* **195,** 827 (1977).